Effect of barrier height on spectral characteristics of GaAs/$Al_xGa_{1-x}As$ QWIP

Hu Xiaoying, Liu Weiguo, Duan Cunli, Cai Changlong, Niu Xiaoling

(Shaanxi Key Laboratory of Optoelectronic Functional Materials and Devices, School of Optoelectronic Engineering, Xi′an Technological University, Xi′an 710032, China)

Abstract: A comprehensive analysis on the relationship between the barrier height and the peak wavelength of bound-to-quasi-continuum Quantum Well Infrared Photodetector (QWIP) was demonstrated, together with its effect on characterization of microstructure and macroscopic optic properties of the device-sample. The GaAs/$Al_xGa_{1-x}As$ infrared quantum well material was produced via the method of Metal Organic Chemical Vapor Deposition(MOVCD). Two sample devices with different Al content(0.23 and 0.32) was designed respectively and their corresponding spectral responses were measured via Fourier Transform Spectrometer at the temperature of 77 K. The experimental results shown that sample 1# and 2# are with the peak wavelengths of 8.36 μm and 7.58 μm, which present obvious difference to the theoretical results based on Schrodinger equation (9.672 μm and 7.928 μm, corresponding to errors of 15.6% and 4.6%, respectively). By analyzing the effect of Al atoms diffusion length, it is found that the decrease of Al content is the key effect which leads to sub-band narrow down and peak wavelength red shift. Meanwhile, by using the method of High Resolution Transmission Electron Microscopy(HRTEM), it is found that the strong error of sample 1# is mainly due to the crystal lattice mismatch between GaAs and AlGaAs, together with the unsatisfied precise control during the growth of quantum well material. Above analysis demonstrates that adjusting the Al content of barrier height is an effective method to turn the peak wavelength of QWIP.

Key words: QWIP; HRTEM; GaAs/$Al_xGa_{1-x}As$; peak wavelength

CLC number: TN215 **Document code:** A **Article ID:** 1007-2276(2015)10-2995-05

势垒高度对 GaAs/$Al_xGa_{1-x}As$ QWIP 光谱特性的影响

胡小英,刘卫国,段存丽,蔡长龙,牛小玲

(西安工业大学 光电工程学院 陕西省光电功能材料与器件重点实验室,陕西 西安 710032)

摘 要: 为了确定束缚态到准束缚态工作模式 QWIP 响应波长与势垒高度关系，采用金属有机物化学气相沉积法生长制备势垒高度不同 GaAs/$Al_xGa_{1-x}As$ QWIP 样品，采用傅里叶光谱仪对样品进行77 K液氮温度光谱测试。结果显示 1#,2# 样品峰值响应波长与据薛定谔方程得到峰值波长误差为 15.6%，4.6%。结果表明:引起量子阱中子带间距离逐渐扩大与峰值响应波长蓝移的根本原因是势垒高度的

收稿日期:2015-02-10； **修订日期:**2015-03-15

基金项目:兵器预研基金项目(62201070821);总装光电专用(40405030104);陕西省重点实验室开放基金(ZSKJ201301);西安工业大学校长开放基金(XAGDXJJ1401);重点院长基金(13GDYJZ01)

作者简介:胡小英(1978-),女,副教授,研究生导师,博士,主要从事红外光电材料与器件方面的研究。Email:490027874@qq.com

增加。高分辨透射扫描电镜实验结果表明量子阱材料生长过程精度控制不够及 AlGaAs 与 GaAs 晶格不匹配是造成 1# 样品误差较大的主要原因。说明调节势垒高度可实现 QWIP 峰值波长微调的目的。

关键词：量子阱红外探测器； 高分辨透射扫描电镜； $GaAs/Al_xGa_{1-x}As$； 峰值波长

0 Introduction

The quantum well infrared photodetector (QWIP) is a novel infrared device, which is combined by advanced film growth and micro-electronics. Because it has such advantages as even thickness, mature preparation technology, low cost, good anti-irradiation properties, easy to implement multi-color detection and so on [1-4]. Recently it has been main stream technology of infrared acquisition aid due to its wide use in the following fields: space resources determination, mines detection, biological and medical imaging, high technology and modern armaments in military arena, infrared guidance systems, battlefield surveillance, thermal transmission microscopy of anti-tank guided missiles and so on[5-7]. Since QWIP was reported last century, it has been made rapid progress. Mature QWIP products have been made abroad from the unit device to the focal plane one, but the research domestic is still relatively poor[8]. Especially with the deep research on sub-band physics and device performance optimization, how to effectively change the peak wavelength of QWIP, and realize multi-channel detection technology has become a hot topic[9], although some methods has been reported which can adjust peak wavelength as laser annealing, QW interface mixing technique, rapid thermal annealing and so on[10-13]. These techniques can change the band gap structure of the original growth material, the QW shape and the well neutron zone, and detected wavelength[14-16], but the process is complex, expensive, and poor controllable. However, the method in the paper is making the excited state in sub-band transmission designed in barrier edge or slightly less than barrier top (quasi bound states) to change the band structure, reduce dark current, realize QW energy level local fine-tuning, and meet needs of different band detection by adjusting barrier height.

1 Information of samples

$GaAs/Al_xGa_{1-x}As$ QW material is grown on semi insulating GaAs in 100 crystal by metal organic chemical vapor deposition(MOCVD). The QW structure of Al absorption layer is 40 cycles, three methyl aluminum(TMAl) is for Al source, and $GaAs/Al_xGa_{1-x}As$ barrier layer is 50.0 nm. The thickness of GaAs well is 5.0 nm. 10% AsH_3 in reaction furnace is for As source. Trimethyl gallium(TMGa) is for Ga source. Si doped concentration is 5×10^{17} cm^{-3}. Absorption layers are 1 000 nm and 1 500 nm *N* type heavily doped GaAs. Si doped concentration is 1.5×10^{18} cm^{-3}. Doped air source is SiH_4. Ohmic contact electrode uses *n* GaAs ohmic contact and multilayer metal structure AuGeNi/Au by stripping and rapid thermal annealing process. Sample device is made by epitaxial growth, design and fabrication. The sample size is 300 μm×300 μm, upper and lower electrode pad area is 80 μm×80 μm and 20 μm×20 μm respectively, located on the photosensitive surface as shown in Fig.1.

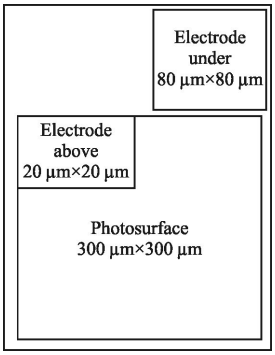

Fig.1 Structure of QWIP sample

2 Experiment

Al content in 1# barrier is 0.23 while the one in

2# is 0.32. They are separately polished at side 45°. Ohmic contact layer of upper and lower electrodes is made of AuGeNi/Au layer. After electrodes are welded by gold wire ball, samples are placed into 77 K liquid nitrogen refrigeration dewar, which is bottled into Fourier spectrometer. Meanwhile, the bias (5.0 V) is given to samples. Preamplifier is used to amplify optical current signal and transmit to data processing system of spectrometer. We can get spectral response curve as shown in Fig.2.

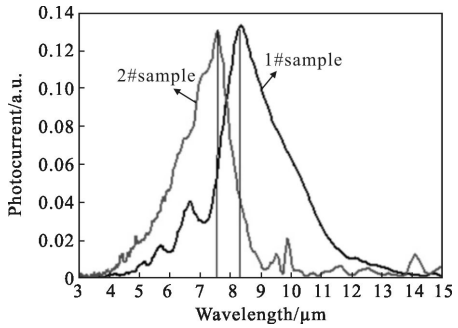

Fig.2 Spectra of 1# and 2# sample

Peak wavelength of QWIP is represented by the following formula:

$$\lambda_p=\frac{hc}{(E_2-E_1)} \tag{1}$$

Where h is Planck constant, c is speed of light. E_2 is the excited level (by Schrodinger equation below), E_1 is well ground level (by the transfer matrix method). Calculation of the energy levels is based on the finite deep square potential well model and effective mass approximation theory. Thus, we can acquire calculated and experimental peak wavelength in Tab.1 under appropriate test conditions.

Tab.1 Comparation between calculated and tested peak wavelength of 1# and 2#

No.	$\Delta E=E_2-E_1$/meV			Wavelength/nm		
	ΔE_c	ΔE_e	ΔE_d	λ_{pc}	λ_{pe}	λ_{pd}
1#	128.2	148.2	20.0	9 672	8 360	1 308
2#	156.4	163.6	7.2	7 928	7 580	347

Subscripts c, e and d are for calculations, experiments and deviation respectively, and λ_p is for the peak wavelength.

3 Experiment analysis

According to the mixing effect of hetero interface expression error distribution function, there is the inevitable phenomenon of hetero junction interface on $Al_xGa_{1-x}As$ and GaAs layer, and the diffusion process has been enhanced in after-processing sample under the main consideration to the surface kinetic processes. According to the diffusion theory, the $x(z)$ of Al can be determined in hetero-structure interface:

$$x(z)=\frac{x_0}{2}\left[2+\mathrm{erf}\left(\frac{z-d_w/2}{2L}\right)-\mathrm{erf}\left(\frac{z+d_w/2}{2L}\right)\right] \tag{2}$$

Where x_0 is the initial of Al atomic concentration in barrier, erf (x) is the residual function, d_w is QW width, L is Al diffusion length, the center is $z=0$ in QW. Atomic diffusion has changed the original square potential well shape and affected peak wavelength.

Al diffusion length can be obtained by comparing the theoretical and experimental values of device cutoff wavelength. According to Fig.2, peak photocurrent of 1# is at 8 360 nm (E_{1e}=148.2 meV) while the one of 2# is at 7 580 nm (E_{2e}=163.6 meV). Al atomic diffusion length of 1# and 2# obtained is 2.1 nm and 2.7 nm respectively. At the same time, the corresponding electronic energy level E_0 computed in ground state is 0.148 eV and 0.163 eV under AlGaAs conduction band edge. And the local Fermi level E_f at 77 K temperature above E_0 is 4 meV and 9 meV (Here kinetic energy carriers are ignored in the xy plane).

From above analysis we can see that, because barrier layer is relatively thick, it is very difficult for electron occupied E_0 in the ground state to escape to other QW. Similarly, according to the complex eigenvalue theory, electron in the ground state of E_0 lives longer, and the probability to escape the state through barrier will be smaller. The GaAs QW can be changed from the square potential well into the shape determined by complementary error by adjusting Al in GaAs/$Al_xGa_{1-x}As$ QWIP to control the extent of diffusion between GaAs and $Al_xGa_{1-x}As$ at the interface

of aluminum atoms. The well depth is reduced while its width is increased, thus the distribution of sub level will be changed, which eventually realize the device response wavelength trimming purposes.

From Tab.1 we can see that: the transition energy of 1# between ground state and excited one is 128.2 meV, and corresponding peak wavelength is 9672 nm, while the one of 2# is 156.4 meV, and corresponding peak wavelength is 7 928 nm. Theoretical value fully proves that increasing Al content will make peak wavelength decrease and the electron transition energy increase.

From Fig.2 we can see: the peak wavelength of 1# is 8 360 nm (the transition energy between ground state and excited one is 148.2 meV), while the one of 2# is 7 580 nm (the one between ground state and excited one is 163.6 meV). Spectral response tested results further verify the correctness of the theoretical calculation. It is found that peak wavelength of 1# and 2# blue shift about 1 312 nm and 348 nm respectively.

Deviation of 1# is 3.78 times larger than 2#. Because the high resolution technique is the most effective method to observe and analyze the interface structure of QW material, which does the research from the micro scale interface structure of GaAs/$Al_xGa_{1-x}As$ material by using electron microscopy, Fig.3 and Fig.4 are 1# and 2# interface of high-resolution image by means of high resolution transmission electron microscopy(HRTEM).

Figure 3 shows that 1# has the obvious dislocation phenomenon in annular region, the author thinks that the dislocation phenomenon will cause lattice mismatch between GaAs and AlGaAs and lead to stress and strain, and the stress strength directly determines the transition energy and the sub size between ground state and excited one. According to spectral test results, it is GaAs and AlGaAs lattice mismatch and the weakened stress that lead to 1# large deviation, which makes the transition energy between ground state and excited one increase and peak wavelength blue shift. From Fig.3 non-uniformity in delta region, we can see that control precision of the sample growth process is not enough, and each interface thickness has fluctuated disorderly in material growth direction, which will affect size and direction of the carrier velocity, and cause transition energy changed between ground state and excited one.

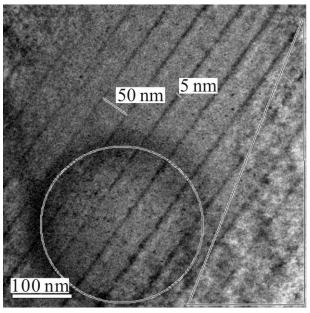

Fig.3 Interface structure of 1#

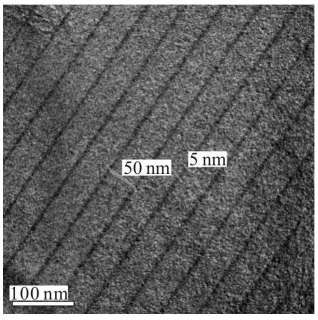

Fig.4 Interface structure of 2#

The main reason causing 1# error much larger is obvious dislocation phenomenon in ring and non-uniformity in delta region. But from Fig.4 it can be seen that control precision of 1# growth process is better than that of 2#, and there is no uneven growth dislocation phenomenon and obvious material in 2#, all these gives the powerful explanation for 2# smaller error. Of course, error caused by testing system and theoretical calculation also has certain effect on them, which only accounts for the non dominant role.

From above analysis and discussion for 1# and 2# sample by HRTEM, according to Fig.2−4, and Tab.1, it can be seen that when the Al fraction x increases, the peak wavelength λ_p moved towards the short wave, this is mainly due to the excited state decreased with reduction of barrier height, which shows that the

excited state gradually moved from well inside to well outside, that′s optical excitation carriers are changing from bound-to-continuum to bound-to-quasi-bound model. And sub-band spacing gradually is reduced. Reducing Al content of the barrier will result in band gap decrease between barrier and well region. In addition, the variation of transition energy between bands caused by changing Al content comes mainly from the electronic energy level of ground state in the conduction band, and has nothing with the width of band gap and hole ground state energy level. The error between the theoretical and tested results, on the one hand is from control precision of the sample growth process and each interface thickness fluctuated disorderly in material growth direction, on the other hand is from the approximate conditions in theoretical calculation.

4 Conclusion

GaAs/$Al_xGa_{1-x}As$ QWIPs were designed, grown and fabricated. Sample devices spectra were tested via Fourier transform spectrometer at 77 K. A comprehensive analysis on the relationship between Al content and peak wavelength has been demonstrated, together with its effect on characterization of microstructure and macroscopic optic properties. By analyzing the effect of Al atoms diffusion length, we found that the decrease of Al content is the key effect which leads to sub-band narrow down and peak wavelength red shift. Meanwhile, by first using the method of HRTEM, we found that the strong error of sample-device is mainly due to the crystal lattice mismatch between GaAs and AlGaAs, together with the unsatisfied precise control during QW material growth. Above analysis demonstrates adjusting Al content of barrier height is an effective method to turn QWIP peak wavelength.

References:

[1] Lu Wei, Li Ning, Zheng Honglong, et al. A new group of infrared opto-electronics-quantum well infrared photodetectors [J]. ***Science in China***, 2009, 39(3): 336-343. (in Chinese)

[2] Li N, Xiong D Y. Dark currents of GaAs/AlGaAs quantum-well infrared photodetectors [J]. ***Appl Phys A***, 2007, 89: 701-705.

[3] Hu Xiaoying, Liu Weiguo, Duan Cunli, et al. Research on dark current of GaAs/$Al_{0.3}Ga_{0.7}As$ quantum well infrared photodetector by HRTEM [J]. ***Infrared and Laser Engineering***, 2014, 43(4): 1057-1060. (in Chinese)

[4] Ergun Y, Hostut M. Broadband staircase quantum well infrared photodetector with low dark current [J]. ***Infrared Physics & Technology***, 2006, 48: 109-114.

[5] Kwong-Kit Choi, Murzy D Jhabvala, David P Forrai, et al. Electromagnetic modeling and design of quantum well infrared photodetectors [J]. ***IEEE Journal of Selected Topics in Quantum Electronics***, 2013, 19(5): 3800310.

[6] Sarath D Gunapala, John K Liu. 9 μm cutoff 256×256 GaAs/AlGaAs quantum well infrared photodetector hand-held camera [J]. ***IEEE Transactions on Electron Devices***, 1997, 44(1): 51-55.

[7] Hu Xiaoying, Liu Weiguo, Duan Cunli, et al. Spectroscopic characteristics of GaAs/$Al_{0.3}Ga_{0.7}As$ quantum well infrared photodetectors [J]. ***Infrared and Laser Engineering***, 2015, 44(8): 2305-2308. (in Chinese)

[8] Gunapala S D, Bandara S V. 640×512 pixel narrow-band, four-band, and broad-band quantum well infrared photodetector focal plane arrays [J]. ***Infrared Physics & Technology***, 2003, 44: 411-415.

[9] Mehjabeen A Khan, Akeed A Pavel, Naz Islam. Intersubband transition in asymmetric quantum well infrared photodetector [J]. ***IEEE Transactions on Nana Technology***, 2013, 12(4): 521-523.

[10] Levine B F, Bethea C G. High detectivity $D^*=1.0\times10^{10}$ cm/Hz·W^{-1} GaAs/AlGaAs multiquantum well $\lambda=8.3$ μm infrared detector[J]. ***Appl Phys Lett***, 1988, 53: 296-300.

[11] Ribet-Mohamed I, Le Rouzo J, Rommeluere S, et al. Advanced characterization of the radiometric performances of quantum well infrared photodetectors [J]. ***Infrared Physics & Technology***, 2005, 47: 119-131.

[12] Dupont E, Byloos M. Pixelless thermal imaging with integrated quantum well infrared photodetector and light emitting diode[J]. ***IEEE photonics Echnology Letters***, 2002, 14(2): 182-186.

[13] Yang Y, Liu H C. Optimal doping density for quantum-well infrared photodetector performance [J]. ***IEEE Journal of Quantum Electronics***, 2009, 45(5-6): 623-626.